On the correlation between hardness and yield strength in multilayered elastic-plastic materials

Y.-L. SHEN*, X. H. TAN
Department of Mechanical Engineering, University of New Mexico, Albuquerque, NM 87131, USA

Nanoindentation has been increasingly utilized for characterizing mechanical properties of small-scale materials and structures. One notable example is multilayered metallic films [1–3]. Concerns have been raised about what the indentation hardness of the composite layers really represents [4]. This study is our first attempt to quantify the indentation hardness of multilayered materials and to correlate it to the overall yield property of the entire structure. For simplicity attention is limited to alternating layers of two metals of equal thickness. Hypothetical elastic-plastic properties of the constituent layers are used as input in the modeling. The indentation displacements considered are sufficiently deep so the effective hardness resulting from the composite structure can be obtained. In particular, we intend to find out if indentation hardness can provide an accurate account of the overall composite flow stress.

The model system is a laminated structure consisting of alternating layers of material A and material B of equal thickness. Both A and B are taken to be isotropic elastic-perfectly plastic. The Young's moduli (E) and Poisson's ratios (ν) are $E_A = 100$ GPa, $E_B = 200$ GPa, $\nu_A = 0.3$ and $\nu_B = 0.3$. The yield strengths σ_y are set to be $\sigma_{y,A} = 50$ MPa and $\sigma_{y,B} = 150$ MPa. Plastic yielding follows the von Mises criterion. All interfaces between adjacent layers are assumed to be perfectly bonded. Note that, although the individual layer thickness may be conceived to be in the sub-macroscopic range, there is no intrinsic length scale involved in the present continuum-based simulation. As a consequence, there is no size-dependent effect caused by the varying underlying deformation mechanisms found in actual micro- and nano-layered metals.

Finite element analyses of compressive loading are first performed to obtain the overall yield strength of the composite, as schematically shown in Figs. 1a and b. Both the longitudinal and transverse loading configurations are considered. In the pure elastic regime, the effective moduli of the laminates thus obtained can be approximated by the simple rule-of-mixtures solutions applied to the isostrain condition for longitudinal loading and the isostress condition for transverse loading. Our main focus here, however, is on the overall yield strength. The calculated composite response will be the "true" effective properties of the entire multilayer structure with all three-dimensional features accounted for.

The effective stress-strain response in the transverse direction is then used as the input response of a *homogeneous* material to be subjected to indentation loading. Since the homogeneous material used here actually represents the multilayers (with the composite material properties built in), the modeled indentation hardness will be the "true" value one would seek when employing the indentation technique on the multilayer structure. (However, we illustrate in this work that, when indentation is applied to a material with the layered structure *explicitly* accounted for, there is a significant deviation of the hardness values from the "true" values.)

Simulations of indentation are based on the axisymmetric model featuring a rigid conical indenter. Fig. 1c shows a schematic of the model. The semi-angle of the conical indenter is 70.3°, resulting in a same projected area as the Berkovich indenter [5–8]. There are a total of 60 alternating layers of material A and material B, all of equal thickness. In Fig. 1c, the topmost layer to be in direct contact with the indenter is shown to be material A. In our analysis another model, with the topmost layer being material B, is also considered. These two multilayer arrangements are henceforth referred to as "AB stack" and "BA stack," respectively. (In the case of indenting a homogeneous material having the built-in composite properties, as described in the previous paragraph, the entire specimen is simply replaced by a homogeneous material with the specified elastic-plastic input response.) The left-hand boundary is the symmetry axis. The total thickness of the specimen is $60t$, where t is the thickness of the individual layer. The lateral span (radius) of the model is $100t$. The left-hand boundary is allowed to move only in the vertical direction. The bottom boundary is allowed to move only in the horizontal direction. The right-hand boundary is not constrained. The top boundary, when not in contact with the indenter, is also free to move. The coefficient of friction between the top layer and the rigid indenter is taken to be 0.1 (which is a typical value for the diamond/metal contact pair [9, 10]). The modeled hardness is defined to be the indentation load divided by the current projected contact area. In calculating the contact area, the last nodal point on the top surface in contact with the indenter is identified so the effect of pileup is readily taken into consideration. The finite element program ABAQUS (Version 6.4, Abaqus Inc., Pawtucket, RI) is employed in all calculations. A total of 65520

*Author to whom all correspondence should be addressed.

0022–2461

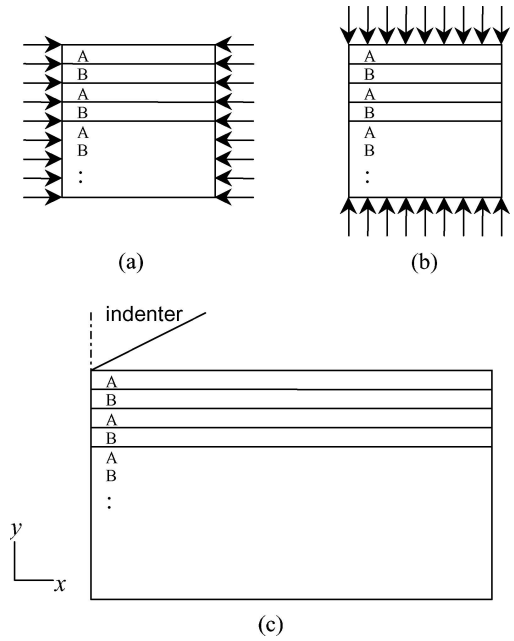

Figure 1 Schematics showing (a) longitudinal and (b) transverse loading configurations, for modeling the overall compressive response of the multilayered composite. (c) The indentation model, where the specimen and indenter both possess axial symmetry about the left boundary. The rigid indenter has a semi-angle of 70.3°.

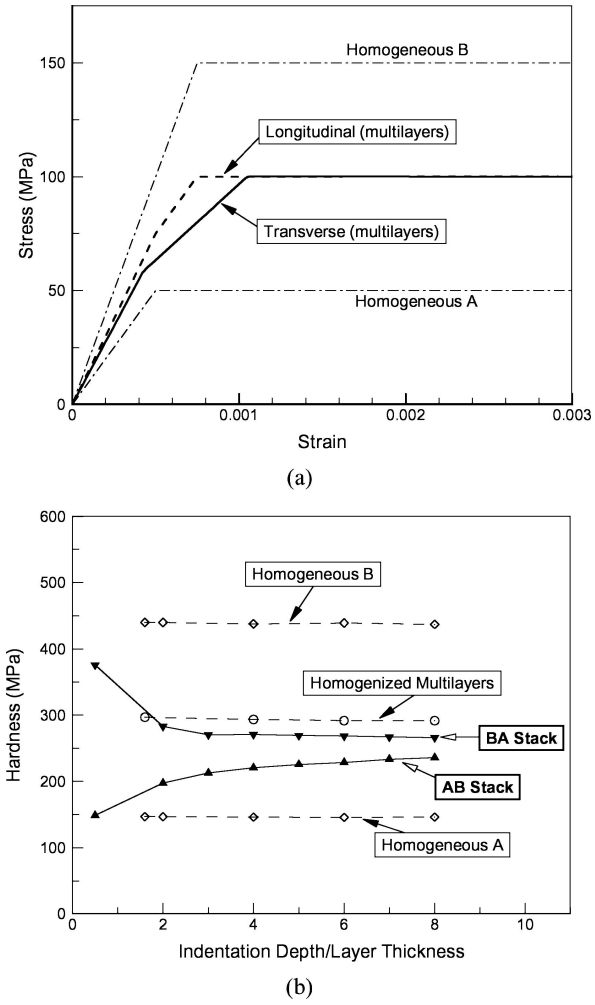

Figure 2 Modeled overall compressive stress-strain curves of the multilayers. Also included for reference are the input stress-strain responses for the homogeneous A and B materials. (b) Modeled hardness as a function of indentation depth (normalized with the initial layer thickness, t).

four-noded rectangular elements are used in the model, with a finer mesh size near the upper-left corner. The smallest element has dimensions of $0.1t \times 0.1t$. The mesh convergence is verified by utilizing a separate coarser-mesh model, and the error in hardness is found to be within 1.1% [11].

Fig. 2a shows the modeled overall compressive stress-strain curves. Results from the longitudinal and transverse loading configurations, as well as those of the homogeneous materials A and B used as the modeling input, are all included. It can be seen that, in both loading configurations, the multilayered composite shows a bilinear response before fully yielded. The first linear segment corresponds to a true elastic state. When the von Mises effective stress in layer A reaches $\sigma_{y,A}$, plastic yielding in A commences while B is still in the elastic state. This leads to the second linear segment. When both layers become plastic, a constant flow stress ensues. This flow stress is defined to be the "composite yield strength." The composite yield strength (100 MPa) is observed to be the average of $\sigma_{y,A}$ (50 MPa) and $\sigma_{y,B}$ (150 MPa) for the present multilayer model with 50–50% volume fractions. Although transverse and longitudinal loadings both result in the same composite yield strength along the compressive axis, the individual stress components in the layers are different. Upon full yielding the algebraic values of the stress components in each layer in the transverse case (where the macroscopic compressive axis is in the y direction) are: $\sigma^A_{xx} = -50$ MPa, $\sigma^A_{yy} = -100$ MPa, $\sigma^A_{zz} = -50$ MPa, $\sigma^B_{xx} = 50$ MPa, $\sigma^B_{yy} = -100$ MPa and $\sigma^B_{zz} = 50$ MPa. In the longitudinal case (where the macroscopic compressive axis is in the x direction), $\sigma^A_{xx} = -50$ MPa, $\sigma^B_{xx} = -150$ MPa, and all other components are either zero or with very small magnitudes.

Attention is now turned to indentation modeling. First, the modeled overall compressive stress-strain curve (Fig. 2a) is used as the input response for a homogenous material, termed "homogenized multilayers" in subsequent discussions. The transverse response is chosen for this purpose, although the longitudinal response yields essentially the same indentation result since the indentation hardness under consideration is dominated by the large-deformation plastic behavior of the composite. The elastic response plays essentially no role in affecting the indentation behavior in the present analysis [11]. Fig. 2b shows the modeled hardness as a function of indentation depth for the homogeneous A and B materials, the homogenized multilayers, and the composite structures with explicit A/B layers. It is seen that the hardness values in all homogeneous and homogenized cases are generally independent of the indentation depth. It is also seen that the model of homogenized multilayers results in hardness values which are almost exactly the averages of pure A and B materials. One can calculate the ratio of hardness/yield strength for the homogeneous materials and homogenized multilayers shown in Fig. 2b. Here, if the hardness values are divided by the respective yield strengths (50 MPa for "homogenous A," 150 MPa for "homogenous B,"

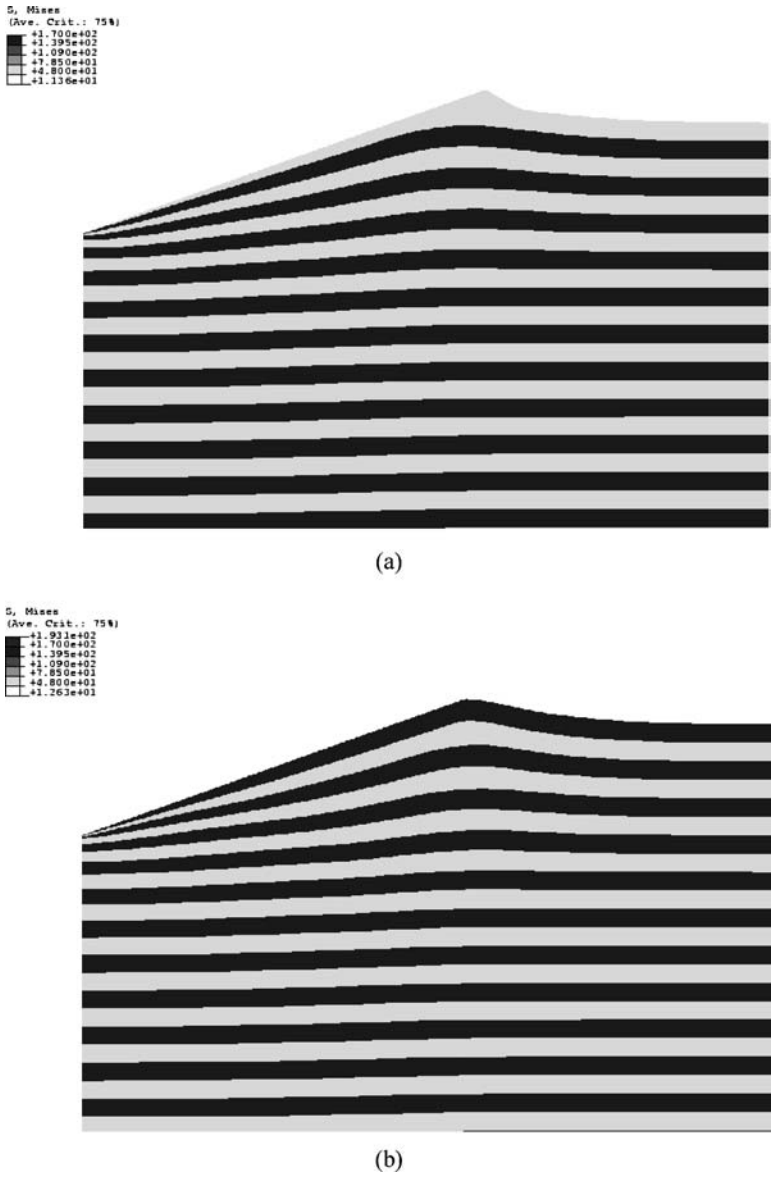

Figure 3 Contours of Mises effective stress (in MPa) in (a) "AB stack" and (b) "BA stack" models, when the indentation depth is at 6t. Only two levels of contour shades are visible because the stresses in the layers have reached the saturation values (50 MPa in A and 150 MPa in B).

and 100 MPa for "homogenized multilayers"), the ratio is approximately 2.93 *for all three models*.

As for the composite structures in Fig. 2b, it is evident that the "AB stack" and "BA stack" models do *not* generate the same hardness results as in the homogenized multilayers. At shallow depths, the hardness is dominated by the top layer material so "BA stack" and "AB stack" result in very high and low hardness values, respectively. As the indentation depth increases the difference from the two arrangements is reduced and the two curves tend to merge. Ideally there will be a single hardness value at very large indentation depths, although in Fig. 2b the two curves are still somewhat apart at a depth corresponding to eight initial layer thicknesses (8t). Nevertheless, it is apparent that both composite models underestimate the overall strength of the structure (recall that the "homogenized multilayers" represents the "true" composite response). For instance, taking the average of the hardnesses of "BA stack" and "AB stack" at the maximum depth in Fig. 2b leads to a value of 251 MPa. Dividing this hardness value by the ratio 2.93 identified above, one obtains the *indentation-derived* composite yield strength of 85.7 MPa, which is about 14% below the "true" composite yield strength of 100 MPa. Therefore, applying indentation on the layered composite clearly leads to an *underestimation* of their overall strength.

Figs. 3a and b show the contours of Mises effective stress in "AB stack" and "BA stack," respectively, when the indentation depth is equal to 6t. For clarity, only the portion close to the indentation is shown. Since no strain hardening is assumed in the constitutive response of A and B, the Mises effective stress reaches a saturation value (50 MPa in A and 150 MPa in B) once plasticity sets in. Therefore, only two levels of contour shades can be seen. Pileups at the edge of the indentation are evident, with the "AB stack" being more distinct because the top layer (A) is the softer of the two. Examining the contours of equivalent plastic strain (not shown here) reveals that very strong plasticity appears underneath the indentation near the interfaces between A and B layers. This implies that severe distortion of material

elements can occur locally if the penetration depth is very large, which could induce numerical problems that prevent the simulations from eventually reaching a converged hardness value for the "AB stack" and "BA stack" models. In an actual multilayered thin-film structure, strong shearing along the interfaces in the region underneath the indentation implies that interfacial sliding and even damage between the layers may occur. The effects of interface features will be left as future work.

One factor that can contribute to the underestimation of composite yield strength by indentation is the localized nature of indentation loading. When overall deformation (such as compressive or tensile testing) is considered, the constituent layers respond to the applied loading as well as the uniform constraint in their respective ways, so the deformation field in each layer is uniform. In the highly localized indentation loading, such type of "ordered" behavior no longer exists. If the several softer layers close to the indent accommodate a greater part of the geometric constraint through easy plastic flow, an underestimation of the uniform composite strength can indeed occur. It should be noted that the present study concentrates only on alternating layers of elastic-perfectly plastic metallic films. If one or both materials strain-harden upon yielding, the indentation response can be significantly influenced depending on the actual material parameters. Nevertheless, the present study serves to provide a baseline understanding of the relationship between indentation hardness and overall yield strength for multilayered elastic-plastic materials. This information is essential for further explorations involving more complex material, geometric, and interface features.

Acknowledgments

This work was partially supported by Air Force Office of Scientific Research under Grant F49620-01-1-0565. Helpful discussions with A. Misra, J. G. Swadener and R. G. Hoagland of Los Alamos National Laboratory are gratefully acknowledged.

References

1. A. MISRA, M. VERDIER, Y. C. LU, H. KUNG, T. E. MITCHELL, M. NASTASI and J. D. EMBURY, *Scripta Mater.* **39** (1998) 555.
2. A. MISRA and H. KUNG, *Adv. Engng. Mater.* **3** (2001) 217.
3. F. SPAEPEN and D. Y. W. YU, *Scripta Mater.* **50** (2003) 729.
4. A. MISRA, J. G. SWADENER and R. G. HOAGLAND, private communications.
5. A. C. FISCHER-CRIPPS, "Nanoindentation" (Springer Press, 2002) p. 20.
6. X. CAI and H. BANGERT, *Thin Solid Films* **264** (1995) 59.
7. M. LICHINCHI, C. LENARDI, J. HAUPT and R. VITALI, *ibid.* **312** (1998) 240.
8. M. MATA, M. ANGLADA and J. ALCALÁ, *J. Mater. Res.* **17** (2002) 964.
9. D. R. LIDE, "Handbook of Chemistry and Physics," 76th ed. (CRC Press, 1995).
10. J. L. BUCAILLE, S. STAUSS, P. SCHWALLER and J. MICHLER, *Thin Solid Films* **447** (2004) 239.
11. X. H. TAN, Master Thesis, University of New Mexico, Department of Mechanical Engineering, 2004.

Received 6 December 2004
and accepted 13 January 2005